Synthesis and Isolation of Cuboctahedral and Icosahedral Platinum Nanoparticles. Ligand-Dependent Structures

Ana Rodriguez, Catherine Amiens, and Bruno Chaudret*

Laboratoire de Chimie de Coordination du CNRS, 205, route de Narbonne, 31077 Toulouse Cedex, France

Marie-José Casanove and Pierre Lecante

CEMES-LOE-CNRS, 29, rue Jeanne Marvig, BP 4347, 31055 Toulouse Cedex, France

John S. Bradley

Max-Planck-Institut für Kohlenforschung, Kaiser-Wilhelm-Platz 1, D45470 Mülheim an der Ruhr, Germany

Received June 13, 1996[⊗]

The reaction of $Pt(dba)_2$ with CO (1 atm) in toluene affords a brown precipitate which can be isolated and redissolved in CH_2Cl_2 to give a colloidal solution of fcc platinum particles with a large size dispersity (10−20 Å, **I**). Redissolution of **I** in THF leads to stable 12 Å fcc platinum particles (**II**) which can be isolated and characterized by high-resolution electron microscopy (HREM) and wide-angle X-ray scattering (WAXS). The original reaction in THF leads to the direct formation of **II**. Addition of 0.2 equiv of PPh_3 to **II** yields a new colloid, **III**, of the same size but of icosahedral structure. **III** was characterized by HREM and spectroscopic techniques. In particular, ^{13}C and ^{31}P NMR spectroscopy demonstrates the absence of a Knight shift for these particles. Addition of excess triphenylphosphine leads to another species, **IV**, displaying broader size distribution with a maximum at 17 Å and an fcc structure. The reaction of **I** with more than 0.2 equiv of PPh_3 affords mixtures containing colloids, clusters (predominantly $Pt_5(CO)_6(PPh_3)_4$), and mononuclear complexes. Both the formation of the colloids and their transformation into molecular species is rapid at room temperature. It is suggested that such processes may be more frequent in organometallic chemistry than previously thought.

Introduction

The physical and chemical properties of materials with particle sizes approaching molecular dimensions, which places them at the frontier between the molecular and the solid state, are of great fundamental interest. These species typically display sizes of the order of 1−2 nm, and the selective synthesis of such materials with well-defined size, structure, and composition is a significant challenge.[1] The preparation of several examples of giant clusters with molecular dimensions in this range has been described by Moiseev and by Schmid et al. who variously obtained Au_{55}, Pt_{309}, Pd_{561}, ..., clusters by partial reduction of inorganic complexes.[2] In all these cases, anionic ligands are present on the clusters, implying a partially oxidized surface. In the specific case of the palladium clusters reported by Schmid[2] and Moiseev[3] the intentional partial oxidation of the surface of the particles is carried out by air oxidation, which apparently stabilizes the clusters.

To explore alternative high yield, easily reproducible syntheses of such species, we have envisaged an organometallic approach. It is well-known that reduction of metal salts by various methods in the presence of polymers leads to sterically protected metal colloids which in certain cases show a narrow size distribution.[4] Organometallic precursors such as Ru(COD)(COT)[5] (COD, 1,5-cyclooctadiene; COT, 1,3,5-cyclooctatriene), $M(dba)_2$ (M = Pd,[5−7] Pt;[7] dba, bisdibenzylideneacetone) or $CpCu^tBuNC$[8] can be decomposed by reactive gases such as CO or H_2 under mild conditions leading to colloids exhibiting narrow size distributions. The isolation of such species under relatively mild conditions is a possible route to the isolation of low-temperature structures and thus materials with unique structure-related properties. In the present study, we use this

[⊗] Abstract published in *Advance ACS Abstracts,* August 1, 1996.

(1) *Clusters and Colloids, from Theory to Applications*; Schmid, G., Ed.; VCH: Weinheim, 1994.

(2) (a) Schmid, G. In ref 1, Chapter 3.3, Metal rich large Clusters with P and N Ligands, pp 178−211. (b) Schmid, G. *Chem. Rev.* **1992**, *92*, 1709. (c) Schmid, G.; Harms, M.; Malm, J. O.; Bovin, J. O.; Van Ruitenbeck, J.; Zandbergen, H. W.; Fu, W. T. *J. Am. Chem. Soc.* **1993**, *115*, 2046.

(3) Vargaftik, M. N.; Zagorodnikov, V. P.; Stolyarov, I. P.; Moiseev, I. I.; Kochubey, D. I.; Likholobov, V. A.; Chuvilin, A. L.; Zamarev, K. I. *J. Mol. Catal.* **1989**, *53*, 315.

(4) Bradley, J. S. In ref 1, Chapter 6, The Chemistry of Transition Metal Colloid; pp 459−544.

(5) Bradley, J. S.; Millar, J. M.; Hill, E. W.; Klein, C.; Chaudret, B.; Duteil, A. *Faraday Discuss. Chem. Soc.* **1991**, *92*, 255.

(6) Bradley, J. S.; Hill, E. W.; Behal, S.; Klein, C.; Chaudret, B.; Duteil, A. *Chem. Mater.* **1992**, *4*, 1234.

(7) Duteil, A.; Queau, R.; Chaudret, B.; Mazel, R.; Roucau, C.; Bradley, J. S. *Chem. Mater.* **1993**, *5*, 341.

(8) (a) Duteil, A. Thèse de l'Université Paul-Sabatier, Toulouse, France, 1992. (b) De Caro, D.; Wally, H.; Amiens, C.; Chaudret, B. *J. Chem. Soc., Chem. Commun.* **1994**, 1891.

S0897-4756(96)00338-9 CCC: $12.00

Table 1. Specific Data for Different Colloids I−IV

colloid	structure	mean size (Å)	IR data (cm^{-1})	most likely formulation
I	cuboctahedral	15	2060 (s), 1884 (m), CH_2Cl_2	$Pt_x(CO)_y$
II	cuboctahedral	12	2050 (s), 1808 (w), THF	$Pt_x(CO)_y(THF)_z$
III	icosahedral	12	2040 (s), THF	$Pt_x(CO)_y(PPh_3)_z(THF)_w$
IV	cuboctahedral	17	2030 (s), THF	$Pt_x(CO)_y(PPh_3)_z$

method to attempt the preparation of metal particles stabilized not by polymers but by classical ligands of organometallic chemistry (CO, PR_3, solvent). However, in this case the formation of molecular complexes during the reactions is a potential complication. In their highly divided form, metals are susceptible to reaction with ligands such as CO. The transformation of platinum colloids into small molecular clusters has been reported in the reaction of CO and water with small platinum colloids.[9] Furthermore the isolation of large molecular clusters showing a definite architecture has been previously reported in particular by Longoni[10] and by Teo,[11] whereas the catalytic properties of some platinum and ruthenium derivatives were proposed by Lewis[12] to be due to the formation of colloids. The ligands we use in the present study are ubiquitous in large transition-metal cluster chemistry.

The potential variation of chemical and physical properties of colloidal metals as a function of their size, size dispersity, and structure requires precise knowledge of size and structure if these properties are to be understood. Small metal particles are known to present well-defined structural types with cuboctahedral, icosahedral, or decahedral morphologies being common.[13−16] The occurrence and frequency of these different types depend on several factors. For example, particle morphologies with apparent 5-fold symmetry are found in the smaller particle size range, arising as they do from strained polytetrahedral twinning, which cannot be maintained at larger particle sizes. At these sizes, although multiply twinned particles are commonly found, the lattice structure of the particles or its subunits is usually that of the elemental metal. Since particle size is the most obvious variable observed as synthesis conditions are changed, particle structure is also likely to be synthesis dependent. The unpredictability of small particle structure and morphology makes it necessary to determine as precisely as possible these parameters. In the present study we have identified these parameters by both transmission electron microscopy (TEM) and high-resolution TEM (HREM) lattice imaging techniques. Wide-angle X-ray scattering (WAXS) measurements[17,18] provide an alternative method to determine the structure and size distribution of particles in some samples, in particular in the case where the particles were very small or suffered beam damage or other instabilities in the TEM experiments.[18]

Scheme 1. Synthesis and Interconversion of Colloids I−IV

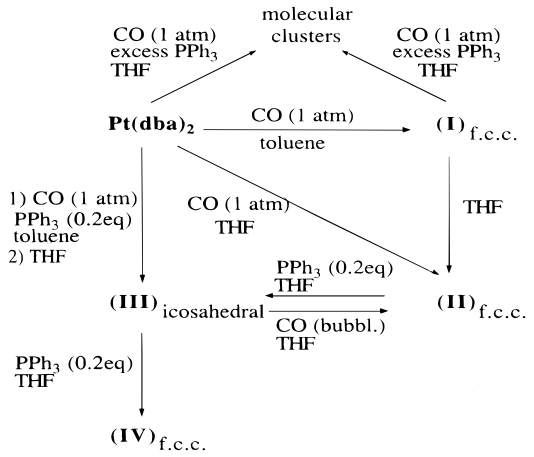

We report here the synthesis and characterization of small platinum particles stabilized only by carbon monoxide, phosphine ligands, and solvent, together with their transformation into molecular clusters. A preliminary account of part of this work has been published.[19]

Results and Discussion

Reaction of $Pt(dba)_2$ with Carbon Monoxide. *Synthesis.* The reaction of solutions of $Pt(dba)_2$[20] with CO has previously been used as a source of small supported metal particles when carried out in the presence of graphite[21] or of colloidal solutions containing 10 or 15 Å particles when a stabilizing polymer, nitrocellulose or cellulose acetate, was added in the solution.[7] We have investigated this reaction in two solvents, THF and toluene, but in the absence of polymer stabilizers.

The reaction of $Pt(dba)_2$ in toluene under 1 bar of CO leads rapidly to a reddish brown precipitate **I**. The IR spectrum of a Nujol mull of the brown powder obtained after filtration and subsequent washing of the precipitate with pentane shows two strong, broad absorptions in the ν(CO) region at ca. 2060 and 1885 cm^{-1} (see Table 1 and Scheme 1), in agreement with the presence of adsorbed CO in both terminal and bridging geometries. This powder could be partly redissolved in dichloromethane, leaving a very small amount of a dark residue which we assume to be metallic platinum. The IR

(9) Bradley, J. S.; Millar, J. M.; Hill, E. W.; Behal, S. *J. Catal.* **1991**, *129*, 530.
(10) Longoni, G.; Iapalucci, M. C. In ref 1, Chapter 3.2, Low Valent Organometallic Clusters, pp 91−177.
(11) (a) Teo, B. K.; Shi, X.; Zhang, H. *J. Am. Chem. Soc.* **1993**, *115*, 8489; (b) **1992**, *114*, 2743; **1991**, *113*, 4329.
(12) (a) Lewis, L. N.; Lewis, N. *J. Am. Chem. Soc.* **1986**, *108*, 722; (b) *Chem. Mater.* **1989**, *1*, 106. (c) Lewis, L. N. *J. Am. Chem. Soc.* **1990**, *112*, 5998.
(13) Kirkland, A. I.; Jefferson, D. A.; Tang, D.; Edwards, P. P. *Proc. R. Soc. London A* **1991**, *434*, 279.
(14) Malm, J.-O. Thesis, HREM Studies of Supported Metal Particles, 1991, University of Lund, Sweden.
(15) Buffat, P.-A.; Flüeli, M.; Spycher, R.; Stadelmann, P. A.; Borel, J. P. *Faraday Discuss.* **1991**, *92*, 173.
(16) Marks, L. D. *Philos. Mag. A* **1984**, *49*, 81.
(17) Debye, P. *Ann. Phys. (Leipzig)* **1915**, *46*, 809.
(18) Vogel, W.; Rosner, B.; Tesche, B. *J. Phys. Chem.* **1993**, *97*, 11611.
(19) Amiens, C.; De Caro, D.; Chaudret, B.; Bradley, J. S.; Mazel, R.; Roucau, C. *J. Am. Chem. Soc.* **1993**, *115*, 11638.
(20) Moseley, K.; Maitlis, P. M. *J. Chem. Soc., Chem. Commun.* **1971**, 982.
(21) (a) Richard, D.; Gallezot, P.; Neibeker, D.; Tkatchenko, I. *Catal. Today* **1989**, *6*, 171. (b) Gallezot, P.; Richard, D.; Bergeret, G. In Novel Materials in Heterogeneous Catalysis, ACS Symp. Ser. No. 437; Baker, R. T. K., Munell, L. L., Eds.; American Chemical Society: Washington DC, 1990; pp 150−159.

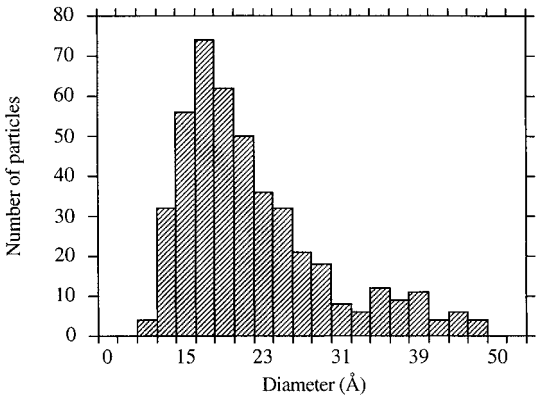

Figure 1. Typical histogram for the size distribution of colloid **I**.

spectrum of the dichloromethane solution shows a strong absorption in the ν(CO) region at 2060 cm^{-1} and another of medium intensity at ca. 1885 cm^{-1}. These spectra are similar to those obtained in solution for 15 Å Pt particles stabilized with nitrocellulose,[7] and terminal CO stretching frequencies have been found near 2035 cm^{-1} for adsorbed CO on very small platinum colloids (<8 Å)[9] and near 2065−2070 cm^{-1} for 30 or 60 Å hydrosols.[22] The vibrational frequencies for CO coordinated to platinum colloids do not appear to vary rationally as a function of the size of the metal particles.

TEM and HREM studies of samples prepared from a CH_2Cl_2 solution of **I** reveal the presence of fcc particles showing a relatively large size distribution (see Figure 1) centered near 15 Å. Although a wide particle size distribution was observed, particles of 12, 15, and 20 Å all showed an fcc structure. For example, Figure 2 shows two such platinum particles: one fcc platinum particle observed along a [110] zone axis and displaying a quasi-perfect cuboctahedral shape (left). The 2.3 Å spacing of the two sets of (111) planes are indicated in the figure. To improve the quality of the displayed micrograph and enhance the definition of the regular (111) and (100) facets, some image processing consisting of high-pass filtering in order to lower the contrast of the background, followed by slight smoothing of the image, was applied. The particle on the right of Figure 2 displays the typical mean size of **I**, namely, 15 Å and the fcc structure; such a particle would correspond to 147 platinum atoms in a closed-shell structure.

When **I** is dissolved in THF under argon, the IR spectrum changes in the νCO region and two bands appear at 2050(s) and 1808(w) cm^{-1} corresponding to a new species, **II** (see Scheme 1). When $Pt(dba)_2$ is decomposed directly in THF under 1 bar of CO, in addition to a small amount of a dark precipitate which was insoluble in common solvents and that we assume again to be metallic platinum, a greenish brown solution is obtained. The IR spectrum of the solution shows four absorptions in the ν(CO) region: 2060 and 2050 (strong), 1885 (medium), and 1808 cm^{-1} (weak). The absorptions at 2060 and 1885 cm^{-1} correspond to **I**, whereas those at 2050 and 1808 cm^{-1} correspond to **II**. After evaporation of the solvent and washing of the brown residue with pentane, the IR spectrum of a Nujol mull of the resulting powder shows a broad strong absorption at ca. 2053 cm^{-1}, a strong absorption at 1884 cm^{-1}, and a weak absorption at 1808 cm^{-1}. The band at 2053 cm^{-1} probably results from the overlap of the bands observed at 2060 and 2050 cm^{-1} in solution due to line broadening in the solid state. The powder could be redissolved in THF, and the solution of **I** and **II** thus obtained is stable under a CO atmosphere; however, after 15 min under argon, only the two characteristic infrared absorption bands of **II** were observed (2050 cm^{-1}, s; 1808 cm^{-1}, w).

TEM studies on solutions of **II**, prepared either directly in THF or after evolution in THF of **I**, reveal the presence of very small fcc platinum particles of 12 Å mean diameter with a narrow size distribution (see Figure 3 and Table 1). However, the particles were found both to be very mobile on the graphite surface under the electron beam and to display a low contrast on the HREM images due to their small size. This led to the observation of only two or three planes in the favorable cases. To have a better characterization of **II**, we used a complementary technique to HREM, namely, WAXS. This technique has been recently used by Vogel et al. to ascertain the structure of gold clusters.[18] The powder obtained by evaporation of the solution of **II** exhibited an amorphous pattern using Mo Kα radiation (0.7107 Å). One important aspect of the molybdenum radiation when compared to copper radiation as used by Vogel is that its shorter wavelength significantly increases the cutoff value for the scattering vector s ($s = 4\pi \sin\theta/\lambda$), which reduces truncation effects in case of Fourier transform and allows for radial distribution function (RDF) analysis. The data collected on a CAD-4 diffractometer were reduced[23] (Figure 4) and then Fourier transformed (Figures 5 and 6). The radial distribution function thus obtained includes well-defined peaks up to an interatomic distance of 10 Å, which provides a direct indication of the size of most particles. Further analysis requires the computation of simulated scattering functions which can be obtained for a given structural model using the Debye formula:

$$i(s) = 2\sum_{i=1}^{N-1}\sum_{j=i+1}^{N} f_i(s)\, f_j(s)\, \frac{\sin(sr_{ij})}{(sr_{ij})} \exp(-b_{ij}s^2)$$

where N is the total number of atoms in the model, f_i the atomic scattering factor for atom i, r_{ij} the distance between atoms i and j, and b_{ij} a dispersion factor affecting the $i-j$ interaction, computed as the sum of individual b_i and b_j dispersion factors. Simulated RDF obtained for 55-atom (two shell) models for both icosahedral and cuboctahedral particles (Figure 5) unambiguously indicated an fcc structure for **II**. A good agreement between experimental and simulated data was obtained both in direct (Figure 6) and in reciprocal space (Figure 4) for a model including a mixture of 55-atom and 147-atom fcc particles in a particle ratio of 90:10 (±5). It is noteworthy that it was necessary to decrease the mean platinum−platinum distance in the model to 2.732 Å and to increase the dispersion factor b_i to 0.01 $Å^2$, which indicates that compared to the bulk, distances in our particles are shrunk by approximately 1.5% and disordered. The models did not include any contribution from the CO ligands, which may partly

(22) Mucalo, M. R.; Cooney, R. P. *J. Chem. Soc., Chem. Commun.* **1989**, 94.

(23) Lecante, P.; Mosset, A.; Galy, J. *J. Appl. Crystallogr.* **1985**, *18*, 214−218.

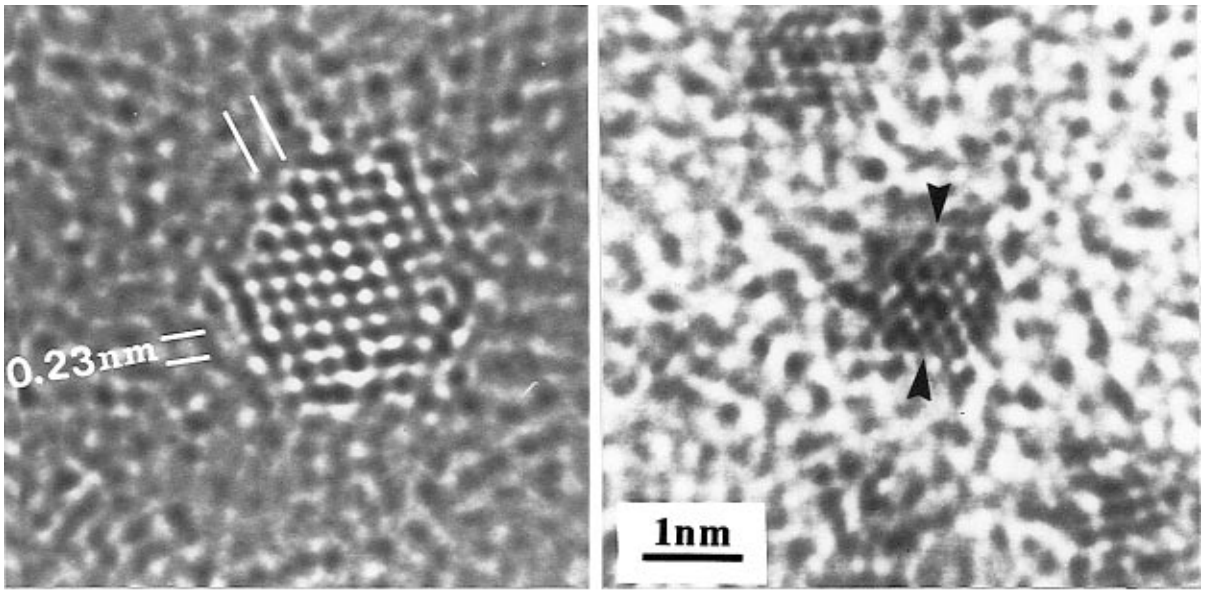

Figure 2. HREM image of two cuboctahedral particles of **I**; respectively, ca. 20 Å (left) and 15 Å (right).

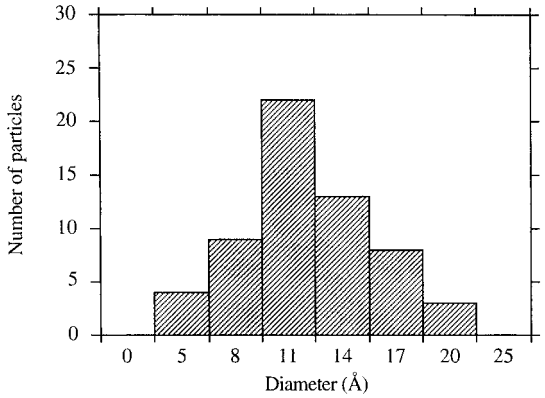

Figure 3. Typical histogram for the size distribution of colloid **II**.

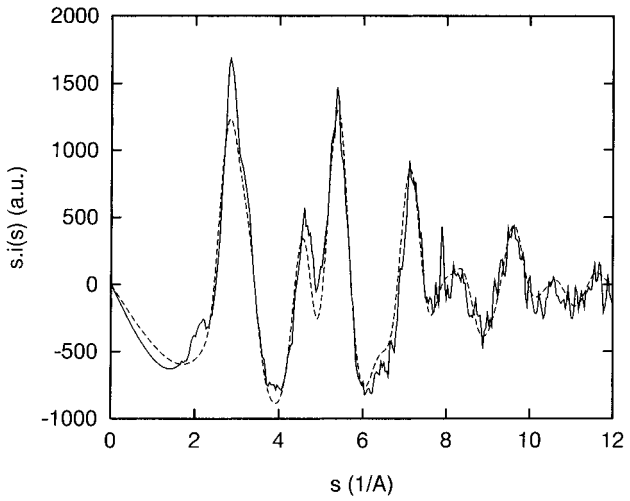

Figure 4. Reduced intensity of particles of **II**: solid line, experimental data; broken line, function simulated from mixed size particle model.

explain the discrepancy observed for interatomic distances below 2 Å.

From these results we conclude that the decomposition of $Pt(dba)_2$ leads first to a colloidal suspension **I** which can be formulated as $Pt_x(CO)_y$. In the absence of carbon monoxide **I** quickly rearranges in THF to **II**. When the reaction is conducted directly in THF a

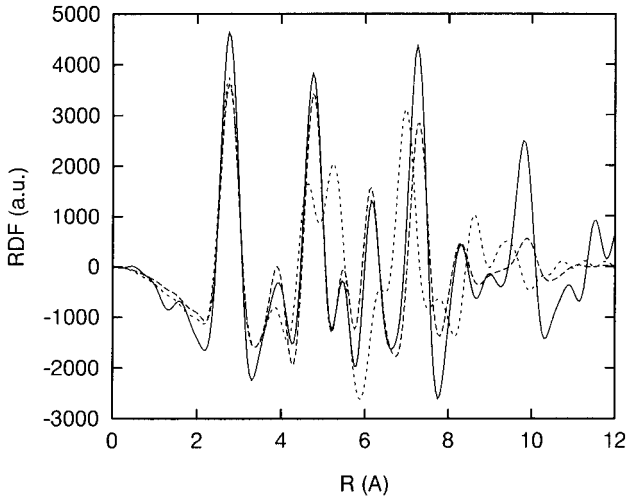

Figure 5. RDF of particles of **II**: solid line, experimental data; thick broken line, cuboctahedral model; thin broken line, icosahedral model.

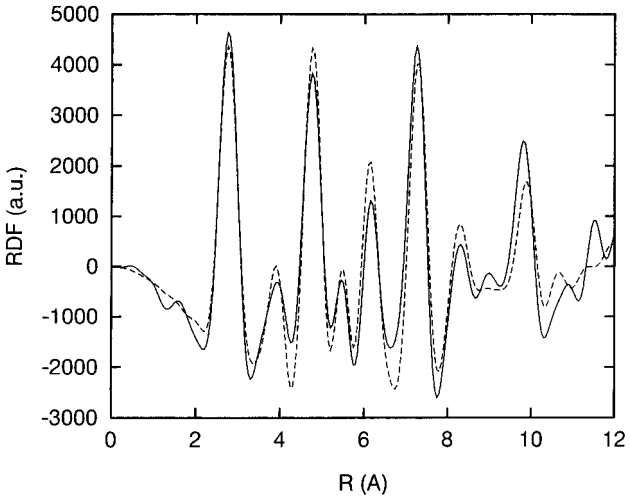

Figure 6. RDF of particles of **II**: solid line, experimental data; broken line, function simulated from mixed size particle model.

mixture of **I** and **II** is initially obtained which then converts to the single final product **II**. The low-frequency shift observed for the CO stretch in **II**

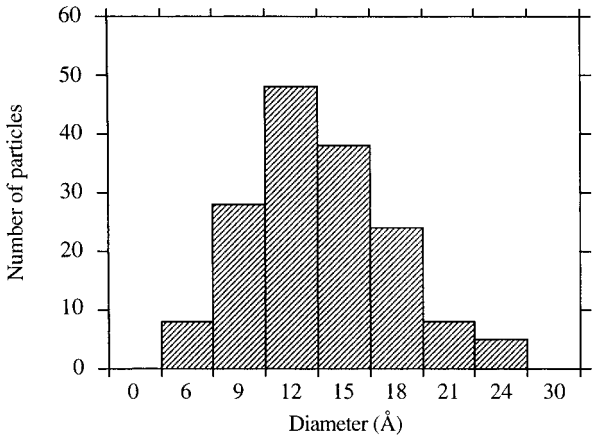

Figure 7. Typical histogram for the size distribution of **III**.

probably reflects the coordination of a basic ligand on the colloidal metal surface rather than a size modification.[24] We thus propose that THF coordination on **I** induces the formation of **II**, which we formulate as $Pt_x(CO)_y(THF)_z$. The relatively large dispersity observed in TEM images of colloid **I** compared to colloid **II** suggests that, under the influence of THF coordination, the polydisperse colloid **I** reequilibrates to a bimodal distribution of more monodisperse (and therefore probably preferred) particles with diameters of 12 and 16 Å. In light of the proposed higher stability for closed-shell clusters, we suggest that **II** contains predominantly closed-shell clusters of 55 atoms, mixed with a low and variable amount of 147-atom clusters, stabilized by coordination with CO and THF molecules.

*Reaction of **II** with Triphenylphosphine.* The reaction was initially carried out by adding 0.1 equiv of PPh_3 to the solid obtained when **I** is dried under reduced pressure and dissolving the mixture in THF under argon. The reaction was monitored by infrared spectroscopy and TEM analysis. **II** is the major species found in solution at the beginning of the reaction as evidenced by the strong absorption at 2050 cm^{-1}, but new bands appear in the spectrum within 15 min at ca. 2020−2017(s) and 1809−1810(m) cm^{-1}. The corresponding products are unidentified molecular species which eventually transform into $Pt_5(CO)_6(PPh_3)_4$ (vide infra). Further addition of 0.1 equiv of triphenylphosphine led to the total transformation of **II** within 1 h into a new product **III**, which displays a single strong absorption at 2040 cm^{-1} in its infrared spectrum. The shift to low frequency of the ν(CO) band observed in the IR spectra of adsorbed CO on **III** compared to those of **I** and **II** is in agreement with the presence of coordinated phosphine ligands.

The addition of 0.2 equiv of triphenylphosphine to a purified sample of **II** in THF under argon at room temperature leads after 5 min to **III** exclusively. Precipitation from pentane afforded a dark brown powder which could be redissolved in THF. **III** is stable in solution under argon but under 1 bar of CO is totally converted into **II** after 2 h as monitored by infrared spectroscopy (see Scheme 1).

TEM analysis of **III** shows a very narrow size distribution centered at 12−13 Å (cf. Table 1 and Figure 7). Unlike the particles in **I** and **II**, the structure shown by particles in **III** is not fcc. Thus no typical planes of this structure could be seen on different micrographs. However, in several cases, an icosahedral structure could be distinguished. Figure 8 shows a representative particle imaged under high-resolution conditions which displays a low contrast as expected for a noncrystallographic arrangement[25] but on which the 5-fold axis characteristic of an icosahedral morphology could be observed. The reason for this structural change is not known, but the two core structures are in fact interconvertible by rotation of the triangular faces around the normal vectors. This relationship between icosahedral and cuboctahedral geometries has been described by Mackay,[25] who showed that in a 55-atom icosahedron, the 42-atom outer shell is not close-packed and displays an interatomic distance 1.0515 times the sum of the atom radii. Such an arrangement might be stabilized sterically by the presence of bulky triphenylphosphine ligands at the surface. It is in this respect interesting to note that samples of the giant cluster of similar size $Au_{55}Cl_6(PPh_3)_{12}$ were also shown to contain predominantly icosahedra by WAXS.[18]

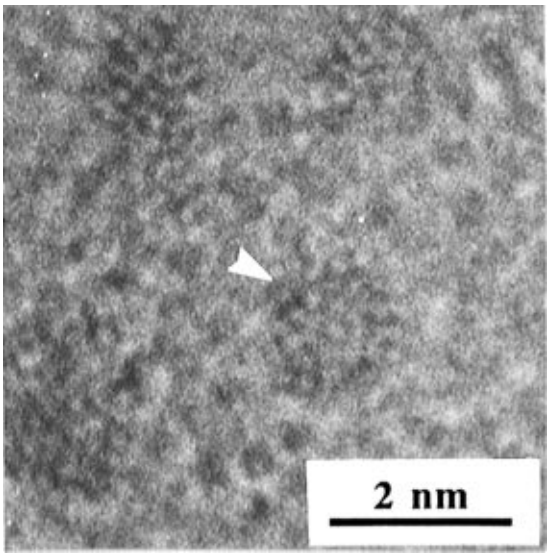

Figure 8. HREM image of a 12 Å icosahedral particle of **III**.

The NMR chemical shifts of ligand atoms coordinated to metal particles can be diagnostic of the electronic structure of the underlying particle. For example, palladium and platinum have large Knight shifts in the metallic state,[26] and this is reflected in the large shifts induced in resonances for nuclei of atoms directly bonded to these metals. Thus solid-state ^{13}C NMR experiments performed on CO adsorbed on platinum clusters either on silica or in a zeolite give results reflecting the metallic nature of the larger silica-supported particles, which induces a strong Knight shift in the CO resonances found at 360 ppm.[27] On the other hand the smaller zeolite entrapped particles are submetallic and show CO shifts of 208 ppm, in the region expected for diamagnetic carbonyl complexes. Simi-

(24) Quéau, R.; Poilblanc, R. *J. Catal.* **1972**, *27*, 200.

(25) Mackay, A. L. *Acta Crystallogr.* **1962**, *15*, 916.

(26) (a) Carter, G. C.; Bennett, L. H., Kahan, D. J. *Metallic shifts in NMR*; Pergamon, Oxford, 1977; Part I, Volume 20, Progress in Material Science; (b) Van der Klink, J. J. *J. Phys. Condens. Matter* **1995**, *7*, 2183. Tong, Y. Y.; Laub, D.; Schulz-Ekloff, G.; Renouprez, A. J.; Van der Klink, J. J. *Phys. Rev. B* **1995**, *52*, 8407.

(27) Sharma, S. B.; Laska, T. E.; Balaraman, P.; Root, T. W.; Dumesic, J. A. *J. Catal.* **1994**, *150*, 225.

larly, the room-temperature ^{13}C chemical shift of CO adsorbed on Pd/SiO_2[28] is 750 ppm. CO coordinated to 70 Å colloidal palladium resonates at almost 800 ppm,[29] but colloidal platinum with 10 Å diameter shows no Knight shift for adsorbed CO.[9]

Since **III** contains two NMR active nuclei in the ligand shell, we were able to apply both $\{^1H\}^{13}C$ NMR and $\{^1H\}^{31}P$ NMR to the analysis of 100% ^{13}CO samples. However, in either case, only very broad signals are observed both at room temperature and at −72 °C, respectively at 170−230 ppm ($\{^1H\}^{13}C$ NMR) and at 10−25 ppm ($\{^1H\}^{31}P$ NMR). The ^{31}P NMR signal is sometimes too broad to be observed, and no peak for free PPh_3 is visible. The presence of phosphine in the solution, whether free or coordinated to the surface of particles, is however attested in ^1H NMR by a broad peak centered at 7.5 ppm for the phenyl protons. We assign the observed resonances respectively to ^{13}CO and PPh_3 coordinated to the surface of the particles. The fact that these chemical shifts are in the normal range for diamagnetic platinum carbonyl and phosphine complexes indicates the absence of Knight shift despite the large known Knight shift for platinum. Since exchange cannot account for the broad signals observed in the $\{^1H\}^{13}C$ and $\{^1H\}^{31}P$ NMR spectra, we favor an explanation based on the heterogeneity of the coordination sites of CO and PPh_3 on the platinum particles. The lack of a large shift for coordinated CO in the present study suggests that our particles have not yet reached the metallic state either as a result of their small (12.6 Å) size or due to perturbations caused by the presence of phosphine ligands on their surface.

We therefore propose that carbon monoxide (and even THF) present on **II** can be reversibly replaced by triphenylphosphine at the surface of the platinum particles to yield **III** which can be described as $Pt_x(CO)_y(PPh_3)_z(THF)_w$ (see Scheme 1). It is important to mention that this easy reaction involves a structural change from cuboctahedral to icosahedral.

When **III**, either an isolated sample or a sample formed in situ upon reacting **I** with 0.2 equiv of PPh_3 in THF, is reacted with an additional 0.2 equiv of PPh_3, a new product **IV** can be detected in the solution by the presence of a strong absorption at 2030 cm^{-1} in the infrared spectrum. TEM analysis of this product shows the presence of platinum particles displaying a relatively broad size distribution centered near 17 Å (see Figure 9 and Table 1) whereas HREM demonstrates that the structure of all particles, whatever their sizes, is cuboctahedral (fcc). Figure 10 shows one of these particles displaying neat facets, observed along a [110] zone axis, together with another fcc particle in which only one set of (111) planes is parallel to the direction of observation. Evidence of strong faceting is given in Figure 11, where the displayed particle lies at the edge of a hole. The driving force for the rearrangement of **III** into **IV** is not understood.

These experiments demonstrate that colloids of different coordination spheres and structures can be prepared by successive substitution reactions from initial platinum particles stabilized only by carbon monoxide. In the next section, we report the direct synthesis of platinum carbonyl phosphine particles.

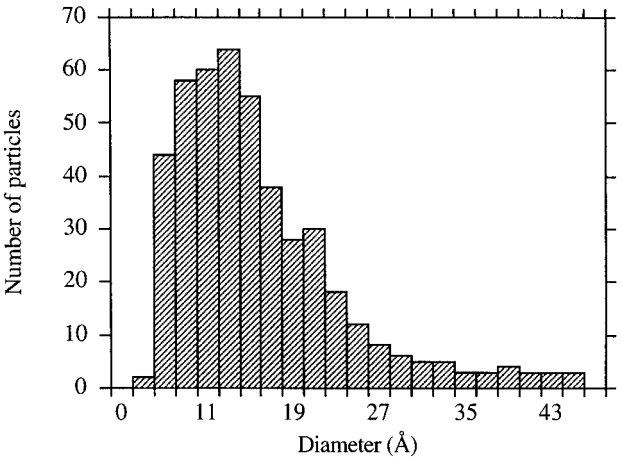

Figure 9. Typical histogram for the size distribution of **IV**.

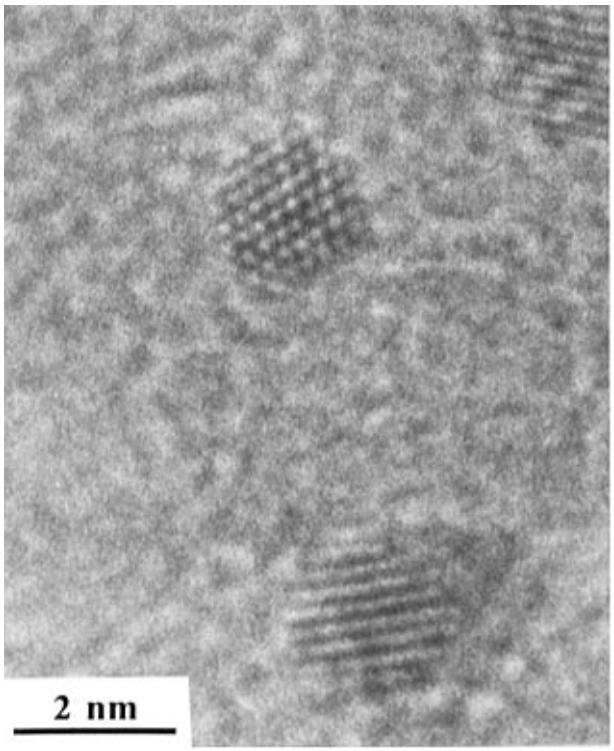

Figure 10. HREM image of a ca. 20 Å cuboctahedral particle of **IV**.

Carbonylation of $Pt(dba)_2$ in the Presence of Triphenylphosphine. *Carbonylation of $Pt(dba)_2$ in the Presence of 0.2 equiv of Triphenylphosphine.* When $Pt(dba)_2$ is decomposed under 1 bar of CO in a toluene solution containing 0.2 equiv of PPh_3, a dark precipitate is obtained which can be purified by filtration. Subsequent washing with toluene and pentane eliminates free dba and unreacted PPh_3. The infrared spectrum of this material recorded in Nujol displays two sets of bands, respectively, at 2060 (s) and ca. 1880 (m) cm^{-1} (attributable to **I**) and at 2040 (s) cm^{-1} (attributable to **III**). The intensity ratio between these two sets of bands varies from experiment to experiment but both are always present in the precipitate spectrum. The product could be redissolved in THF to give a brown solution the infrared spectrum of which is very similar to that in Nujol, but with the expected line narrowing. The evolution of this spectrum with time shows that after 2

(28) Zilm, K. W.; Bonneviot, L.; Simonsen, D. M.; Webb, G. G.; Haller, G. L. *J. Phys. Chem.* **1990**, *94*, 1463.
(29) Bradley, J. S.; Millar, J. M.; Hill, E. W. *J. Am. Chem. Soc.* **1991**, *113*, 4016.

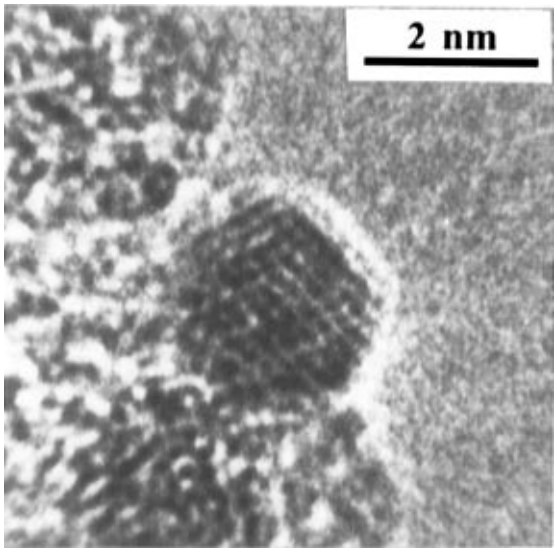

Figure 11. HREM image of a 20 Å cuboctahedral particle of **IV** showing faceting.

h only **III** is present, and consistent with this observation, TEM analysis of this solution shows platinum particles with a narrow size distribution centered around 12 Å.

We thus propose that the decomposition of the platinum precursor under CO in the presence of 0.2 equiv of PPh_3 leads first to a mixture of **I** and **III** which then slowly transforms into **III** (**II** being a possible intermediate in this reaction).

$Pt(dba)_2$ was also decomposed in THF in the presence of 0.2 equiv of PPh_3 by bubbling carbon monoxide through the solution for 5 min. As in the previous case the infrared spectrum of this solution is indicative of the presence of both **I** and **III**. A strong broad band is also present at ca. 2020 cm^{-1} together with a medium-intensity band at ca. 1810 cm^{-1}. Free dba is also observed. This solution is stable under a CO atmosphere but transforms within 1 h under argon into **IV**, which probably results from the presence of free triphenylphosphine in the reaction medium. This indicates that the reaction of triphenylphosphine is slow compared to that of the formation of the platinum particles and that the formation of **III** and **IV** involves the intermediacy of **I** and possibly **II**.

Carbonylation of $Pt(dba)_2$ in the Presence of More Than 0.2 equiv of Triphenylphosphine. When the colloids are synthesized using larger amounts of PPh_3, it is possible to observe by infrared spectroscopy new absorption bands between 2000 and 1780 cm^{-1}, together with bands that can be attributed to **III** and **IV**. The relative intensities of these bands vary according to reaction conditions such as the PPh_3:Pt ratio, duration of the reaction and the presence or absence of CO. During the preparation of colloidal solutions or during the subsequent aging of the solutions, we have detected unidentified species having infrared bands near 2017−2020 and 1810 cm^{-1} and near 1875 cm^{-1}. In addition there is a strong absorption near 1795 cm^{-1} attributable to the presence of Pt_3 or Pt_4 clusters, and absorptions at 2000, 1895, 1862, 1817, and 1793 cm^{-1} attributable to $Pt_5(CO)_6(PPh_3)_4$[30] (**V**). In addition two bands at 1992 and 1950 cm^{-1} are attributable to *cis*-$Pt(CO)_2(PPh_3)_2$ (**VI**).[31] The two latter species are always present in aged solutions containing high PPh_3 concentrations, and from these solutions $Pt_5(CO)_6(PPh_3)_4$, **V**, can be crystallized. NMR monitoring demonstrates that **V** is always the predominant species in solution at PPh_3:Pt ratios higher than 0.2. Moreover, when the system is allowed to stand under argon for an extended period of time, only colloid **IV** and cluster **V** can be observed in solution. Cluster **V** can also be prepared pure in high yield by reacting $Pt(dba)_2$ directly in the presence of 0.8 equiv of PPh_3 under a stream of CO; quick filtration of the solution on a silica column allows the isolation of the product. **V** has been previously isolated and characterized by infrared spectroscopy and X-ray crystal structure.[30] ^{31}P and ^{195}Pt NMR data of the closely related complex $Pt_5(CO)_6(PEt_3)_4$ have been mentioned, but the NMR spectra of **V** have not been reported prior to our work.[30c] We confirmed the identity of **V** by single-crystal X-ray diffraction and by ^{13}C, ^{31}P, and ^{195}Pt NMR spectroscopy.[32]

The second complex which we identified at high PPh_3:Pt content (>0.8 equiv) is *cis*-$Pt(CO)_2(PPh_3)_2$ (**VI**). Thus when the colloidal solutions at this phosphine concentration were left under CO atmosphere for extended periods of time, **IV** and **VI** were always the major products formed.

Having identified the ultimate species formed in the system it was of interest to investigate the ease of the colloid/molecular cluster transformation. For this purpose, we followed the evolution of a colloidal solution formed by decomposition of $Pt(dba)_2$ under CO in THF in the presence of 0.2 equiv of PPh_3 in different conditions.

(i) *Under CO*: The initial solution containing mainly **I** and **II** remains unchanged as described above.

(ii) *Under CO, in the presence of excess PPh_3*: On adding excess PPh_3, the initial solution transforms rapidly first into a mixture containing **IV** and the above-mentioned unknown species showing bands at 2017−1809 cm^{-1} then to a mixture of **IV** and **V**. Further addition of PPh_3 leads to the formation of complex **VI** (see Figure 12).

(iii) *Under argon*: The initial solution changes slowly and after 24 h **IV** is the major product observed in agreement with the results described above.

(iv) *Under argon in the presence of excess PPh_3*: The solution shows the same evolution as that already observed under CO but stops at **V**.

If similar reactions are carried out starting from purified **II**, i.e., from isolated small platinum particles, we observed only the formation of **III** and **IV**; upon addition of excess PPh_3 either under CO or under argon, no molecular species are observed. This experiment suggests that the formation of molecular species occurs from **I** and/or from very small platinum particles formed at the early stage of the reaction.

(30) (a) Barbier, J.-P.; Bender, R.; Braunstein, P.; Fischer, J.; Ricard, L. *J. Chem. Res. (S)* **1978**, 230. (b) Bender, R.; Braunstein, P.; Fischer, J.; Ricard, L., Mitschler, A. *New. J. Chem.* **1981**, *5*, 81. (c) Bender, R.; Braunstein, P.; Richert, J.-L.; Dusausoy, Y. *New. J. Chem.* **1990**, *14*, 569. (d) Evans, D. G.; Hallam, M. F.; Mingos, D. M. P.; Wardle, R. W. M. *J. Chem. Soc., Dalton Trans.* **1987**, 1889.

(31) (a) Hartley, F. R. In *Comprehensive Organometallic Chemistry*; Wilkinson, G., Stone, F. G. A., Abel, E. W., Eds.; Pergamon Press: New York, 1982; pp 474−478. (b) Giannoccaro, P.; Sacco, A.; Vasapollo, G. *Inorg. Chim. Acta* **1979**, *37*, L455. (c) Chini, P.; Longoni, G. *J. Chem. Soc. A* **1970**, 1542.

(32) Wally, H.; Amiens, C.; Chaudret, B., manuscript in preparation.

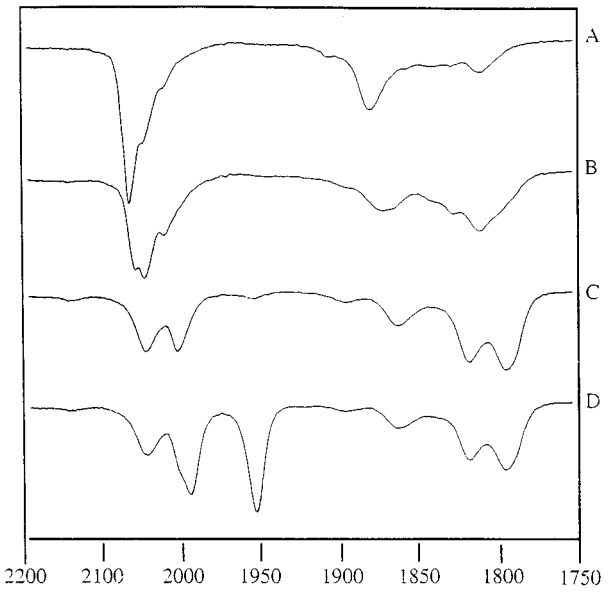

Figure 12. Infrared spectra (cm^{-1}) showing the evolution of a THF solution of $Pt(dba)_2$ under 1 bar of CO containing initially 0.2 equiv of PPh_3 (A) after addition of further 0.2 (B), 0.4 (C), and 0.6 (D) equiv of PPh_3.

Concluding Remarks

The first important result of this study is the demonstration that CO can, by itself or in conjunction with a coordinating solvent, stabilize platinum nanoparticles (12 or ca. 15 Å in diameter). The precipitate first obtained in toluene and containing particles displaying a relatively broad size distribution can be dissolved in THF, leading to crystalline 12 Å particles as detected by TEM. This demonstrates that a coordinating solvent can transform particles into a crystalline material of well-defined size which is an important factor for the understanding of the synthesis of metal particles from metal atoms or monometallic precursors.

The colloids, bearing only CO and presumably solvent molecules, are not very stable with respect to aggregation, and each process of evaporation or precipitation and redissolution is accompanied by the formation of an insoluble black precipitate, probably metallic platinum. In the presence of phosphine, however, better stabilization was achieved and the platinum colloid could be prepared in relatively large quantities and could be isolated and redissolved unchanged. It is interesting to note that the optimum ligand-to-metal ratio for obtaining colloids stable toward precipitation of metal and also toward fragmentation into molecular species is found to be 0.2. Since the size of these colloidal particles, which are approximately equidimensional, is 12 Å, the number of platinum atoms within individual particles must be ca. 55 and therefore the mean number of phosphine ligands per particle should be 11, close to the $M_{55}(X)_x(PPh_3)_{12}$ formulation found to be particularly stable by Schmid. However, we do not propose the formation of molecular giant clusters, a term which implies not only a fixed number of metal atoms and ligands but also a certain geometry of the surface. For the present material, a size distribution is apparent in HREM and only very broad bands appear on the ^{13}C and ^{31}P NMR spectra of our colloids, which we interpret as due to a structural inhomogeneity in the sample. It is nevertheless important to note that no Knight shift is observed on these species. If closed-shell clusters are in fact accessible in this system and are indeed present in the materials we report, purification and isolation procedures remain to be developed to allow their crystallization and structural identification as bona fide molecules.

The second and most important result of this study concerns the structural properties of these colloids which are intriguing since **I**, **II**, and **IV** adopt a cuboctahedral (fcc) structure like bulk platinum itself, whereas **III** adopts an icosahedral structure possibly as a result of the coordination of bulky phosphines.

The final point is the ready transformation of some colloids into small molecular species upon addition of excess phosphine at room temperature to the initial precipitate (**I**), a process for which there does not seem to be any significant kinetic barrier. However, such transformations into molecular species do not easily occur for colloids **II**−**IV**, indicating an inherent stability of these colloids, two of which (**II** and **III**) display a regular size and shape. Since the formation of colloids **I**−**IV** from organometallic precursors is rapid, these experiments also suggest that the nature of the platinum present in a given solution can also change rapidly and dramatically according to the ligand system. This observation could be very important when the ligand system changes with time, as for example during catalytic reactions, thus rendering problematic the identification of active species.

In conclusion, we report in this article the synthesis of small platinum particles of narrow size distribution stabilized by CO alone, CO and THF, or CO, THF, and triphenylphosphine. In contrast to giant clusters obtained by Schmid or by Moiseev, the species described in this study involve only zerovalent platinum; their structure was shown by HREM to be fcc or icosahedral depending upon the ligands present in the coordination sphere. The colloids are stable; they can be isolated and handled like molecular species and can be further used for catalytic or reactivity studies. An interesting point is, however, the ease observed for the transformation between the "molecular" and the "colloidal" state.

Experimental Section

General Methods. All operations were carried out using standard Schlenk tube or Fischer-Porter bottle techniques under argon. Solvents were purified just before use by distillation under nitrogen atmosphere: THF and toluene over sodium benzophenone, pentane over calcium hydride, and dichloromethane over phosphorus pentaoxide.

The colloidal solutions were generally obtained by treating a THF or toluene solution of the platinum precursor, $Pt(dba)_2$, with a stream of CO in a Schlenk tube or in a Fischer-Porter bottle under 1 bar of CO, either alone or in the presence of less than 1 equiv of PPh_3.

TEM specimens of the various colloids were prepared by slow evaporation of a drop of the appropriately diluted solution deposited on a holey carbon film covered grid and ionized. The TEM experiments were performed on a JEM 200 CX-T working at 200 kV and a Philips CM30/ST operating at 300 kV electron microscopes with respective point resolution of 2.3 and 1.9 Å.

Infrared spectra were recorded on a Perkin-Elmer 1725 FT-IR spectrophotometer using colloidal solutions transferred into a KBr cell. The reference spectrum of the solvent was systematically subtracted.

NMR spectra were recorded in benzene-d_6 or toluene-d_8 on a Bruker AMX 400 operating at 400 MHz for ^1H NMR, 161.21

MHz for ^{31}P NMR and 100.71 MHz for ^{13}C NMR. H_3PO_4 80% in D_2O was used to calibrate ^{31}P NMR spectra. In the case of ^{13}C NMR and ^{1}H NMR, the spectra were calibrated using the solvent signals as internal standards, chemical shifts and then given versus TMS.

Materials. $Pt(dba)_2$[20] was prepared according to literature procedures. Dba and PPh_3 were purchased from Aldrich, K_2PtCl_4 from Janssen, and CO from Air Liquide and used without purification.

Colloid I. $Pt(dba)_2$ (50 mg, 0.07 mmol) was dissolved in 12.5 mL of freshly distilled and degassed toluene in a Fisher-Porter bottle. The resulting solution was treated with 1 bar of CO during 10 min under vigorous stirring during which time the solution changed from deep purple to brown and a reddish brown solid precipitated. The solution was removed by filtration and the precipitate was washed with toluene (2 mL) and pentane (2 × 15 mL). IR (Nujol, cm^{-1}): 2060, 1884. TEM data: fcc particles, size: 10−20 Å (Figures 1−4).

Colloid II. I was dissolved in distilled and degassed THF. The solution was stirred for 15 min at room temperature under argon, after which **I** was quantitatively transformed into **II**, which was obtained as a brown solid by precipitation with pentane. IR (THF, cm^{-1}): 2050, 1880. TEM data: fcc crystalline particles, size: 13 Å (±4 Å; Figures 5 and 6).

Colloid III. I was synthesized from $Pt(dba)_2$ (50 mg, 0.08 mmol) as described above. The resulting solid was partially dissolved in 8 mL of THF. After separation of the dark residue by slow filtration, PPh_3 (3.9 mg, 0.016 mmol) was added to the filtrate, and the mixture was stirred for 10 min under argon. **III** was obtained as a brown solid by precipitation with pentane (35 mL). IR (THF, cm^{-1}) 2040. TEM data: icosahedral particles, size: 12−13 Å (Figures 10 and 11).

Colloid IV. This colloid was obtained as described above for **III**, but the mixture was stirred for 4 h at room temperature. IR (THF, cm^{-1}) 2030. TEM data: fcc particles, size ca. 20 Å (Figures 12−14).

Carbonylation of $Pt(dba)_2$ in the Presence of Additional Ligands. $Pt(dba)_2$ (50 mg, 0.08 mmol) and PPh_3 (3.9 mg, 0.016 mmol) were dissolved in 12 mL of toluene, and the mixture was treated with 1 bar of CO. The reaction mixture was stirred for 10 min at room temperature, and a dark precipitate is obtained. After filtration, the precipitate was washed with toluene (2 mL) and pentane (2 × 5 mL). IR (THF, cm^{-1}) 2060, 2040, 1880.

$Pt(dba)_2$ (50 mg, 0.08 mmol) and PPh_3 (3.9 mg, 0.016 mmol) were dissolved into 12 mL of THF. The mixture was stirred for 10 min under a stream of carbon monoxide resulting in a rapid color change from red to brown. IR study of the crude solution shows absorption bands at 2060, 2040, 2020, 1880, and 1810 cm^{-1}.

Carbonylation of $Pt(dba)_2$ in the Presence of >0.2 equiv of Triphenylphosphine. $Pt(dba)_2$ (50 mg, 0.08 mmol) was decomposed by bubbling CO into a THF solution in the presence of 0.2 equiv of PPh_3 (3.9 mg, 0.016 mmol) for 10 min. To this solution was added 0.1 equiv of PPh_3 every 15 min either under CO or under Ar (see text). An infrared spectrum of the solution was recorded after 15 minutes stirring (see Figures 5 and 6).

Acknowledgment. The authors gratefully acknowledge CNRS for support and Rhône-Poulenc for a grant. A.R. thanks Universidad de Castilla la Mancha for financial support.

CM960338L